

# Bridgeless Cuk Converter with Fuzzy Controller for Power Quality Enhancement of PV Integrated EV Charger

G. Niteesh Kumar<sup>1</sup>, Dr. T.Anil Kumar<sup>2</sup>, Dr. G. Venu Madhav<sup>3</sup>

<sup>1</sup> PG Student, Department of Electrical & Electronics engineering, Anurag University, Venkatapur, Ghatkesar MD, Medchal-Malkajgiri District, Telangana, India

<sup>2</sup> Professor, Department of Electrical & Electronics engineering, Anurag University, Venkatapur, Ghatkesar MD, Medchal-Malkajgiri District, Telangana, India

<sup>3</sup> Associate professor, Department of Electrical & Electronics engineering, Anurag University, Venkatapur, Ghatkesar MD, Medchal-Malkajgiri District, Telangana, India

Email: <sup>1</sup>niteesh.gta77@gmail.com, <sup>2</sup>thalluruani@gmail.com, <sup>3</sup>venumadhav@anurag.edu.in

**Abstract:** In this paper, a new output is explored by Bridge Less (BL) Cuk Converter using fuzzy logic controller algorithm for integrated PV electrical vehicle charger (battery). The minimum switch numbers are used to charge the battery at optimum cost in this proposed technique. Stationary voltages and current inputs are achieved despite the unbalanced load operation of the EV-charger i.e. under load, nominal load or overload operation. Also under imbalance of the input supply it retains constant battery parameters. The BL-Cuk converter with fuzzy controller is used to achieve robustness. The proposed technology uses a reduced amount of switching, so the loss of drive is minimal and no DC condenser is required. Therefore, over traditional EV charging approaches, balance voltage is generated across the condenser.

**Keywords:** PV, Bridge less cuk converter, Fuzzy logic controller, EV charger

## 1. Introduction

Battery-powered electric vehicles now dominate the world's transportation infrastructure, paving the way for a sustainable future. An AC-DC converter helps to allow the charging of the electric vehicle battery by inductive charging (EV). In literature with some off-board or on-board topologies, various level 2 or category 3 EV battery chargers are discussed (1-2). A charging station must have improved power quality (PQ) characteristics in conjunction with its high power density and compact form factor to ensure energy efficiency in the charging process (3). The conventional DBR EV Loader, however, draws the peak current from the mains, worsening total harmonic distortion to 55.3% of its source power (THD).

Improved PQ chargers, forming a sinusoidal input line with high pf power and output power, are studied extensively in literature and are tuned stiffenously at a constant value to deal with this problem. In electric vehicle charger discussions, multiple circuit topologies are considered depending on the internal or external configuration (4-5).

Many diverse high-powered on-board loaders with high efficiency have been reported [6-7]. However, off-board setup offers an effective solution due to the reduction of vehicle weight and high power load.

Suitability. The front-end and zero voltage switching are reported in PFC converter topologies in [8-9]. The use of two different inputs has the gain of less ripple current and lower power consumption. Inductor smaller dimension. Thus, the semiconductor devices are treated both at the same time and subsequently, and this results in a decrease in conduction losses. But the interleaved power factor converters do not provide solutions comparable to the conventional power factor converters with power factor correction to the poor thermal use of power factor converters.

An EV charging device including an LLC resonant converter is discussed in a [10] post, which also provides several other benefits. Contrary to note, the complex resonant converter is inadequate to charge EVs at high voltages (11). A full-bridge PFC converter is the most promising solution for e-loaders, but draws too much power and must be built by hand. Various deterministic [12]-[13] PFC off-board EV chargers are discussed in order to ensure ease of implementation, preservation of power density, and efficiency.

Utilizing single- and two-stage PFC conversions, these loaders can be represented using Pi indices. In the literature, several topologies have been reported in single-stage PFC converters with no multiple stages (14). Due to the lower component count, the single-stage charger is more powerful. The presence of destructive 100Hz ripples in the output requires a high capacitance (14). A 2 stage charger with PF correction converter can theoretically handle medium electrical power ratings up to 1 kilowatt. The PFC converter reduces power requirements due to significant loss of electrical power caused by the four input diodes(15). The PFC bridgeless converter offers the most feasible alternative for improving PQ because it performs this role while reducing the number of components involved and minimizing conduction loss. Several unidirectional improved PQ converter are discussed in [16]. In this sense

The buck boost offers the most ideal solution for PFC in EV chargers, which allow the applied input voltage to be bucked (17-18). In [19], we concentrate on reviewing various buck boost converters including buck boost configurations, buck boosts, and SEPIC converters. Although the current input rips are small and the service cycle variations are high, Zeta, Cuk and SEPIC PFC are limited by the SEPIC converters. Cuk converters are also restricted. SEPIC converters aren't always effective. Since low current can be obtained during battery charging, the Cuk Converter provides the most practical charging process (19).

As shown in the figure, several BL Cuk topologies are used with the regular PFC Cuk converter. The literature studies [20-23] address 1(a). The number of components, losses, efficiency and coupling specifications, which are all limited by topologies, are in the paper.

In Figure, topology-1 shown in [20], 1 (b) restricts current, removes EMI, and enables fast implementation. Easy implementation. This product suffers from a saturation issue caused by an interconnection of two intermediate capacitors, C1 and C2, causing more losses on two halves of the output voltage.

Topology-2 employs a variety of components such as two condensers, which can be disadvantageous when used in tiered load routes. Additionally, because the switches for the independent half of the supply voltage are arranged in series, neutral voltage fluctuations occur and can cause floating neutral. 1 1 1 . (d).

Topology-3 in [20] is always a loss, as the body diode of the inactive switch S2 supplies current to the battery diode li2 during the positive half cycle of the input voltage. Two: . (e). Thus, the circuit uses too much energy flipping the inactive switch on and off. Because the existing flow during the second half cycle is partly restored.

A fig is seen in the M-BL Cuk model and in the K-BL Cuk model. 1 (f) and (g) in the same stress as traditional Cuc converter, with reduced semi-conductor modules, and component count much lower than traditional Cuc converter. But connecting a both inductors of each the output and input is not possible for these converters. In turn, this can lead to an increased performance and entrance rip, which for the battery life isn't better.

This work for charging the EV, which meets recommended SAE standard J1772, satisfies the requirement of being a new, improved, bridgless (BL) cucumber converter. The suggested modifications to the loader are summarized as follows to mitigate the above problems.

The medium condenser in both halves helps to minimize circulating losses, increasing the efficiency of the charging voltage.

Due to current flow that won't come back, no current will flow through the body diode of inactive switches. Losses are reduced in the transfer.

The PFC converter uses the same control circuits for every half cycle, which makes it relatively simple to control. The proposed design has ample output inductors to ensure DCM operation, thus reducing the costs and size of the converter.

Contrasting with Fig. In a point-to-point (PtP) BL circuit with a diode in series, the ground-back direction is always available in the line voltage.

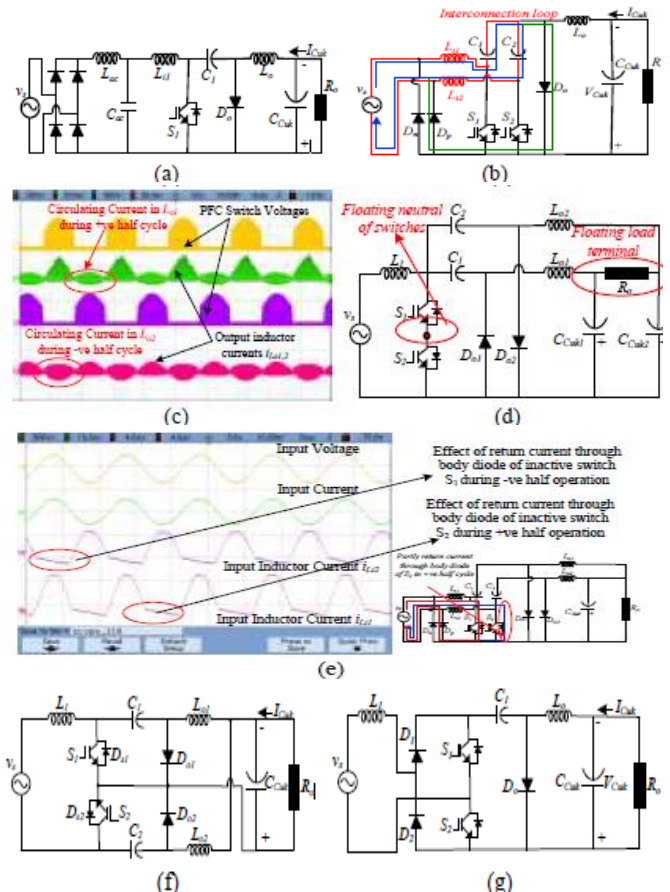


**Fig. 1 Unique BL Cuk converters (a) Common Cuk converters (b) Topology-1 (c) Circuating current Due to interconnection of C1 and C2 in topology-1 (d) Topology-2 (e) topology-3 with return current thurgh body diode (f) topology (g) topology**

There is no floating neutral problem, and additionally, there is little to no EMI noise.

Due to the BL configuration of the proposed converter, which in turn increases the conduction of the electric charge, the losses of the electric charge are decreased. In one switching step the number of components is reduced, resulting in an improvement in charger output from the added converter.

In the next step, the converter turns off the electronic transformer and then adjusts the input voltage to maintain the necessary charging current through the battery in the CC and CV loading areas. Due to its continuous state and its wide range of AC voltage outputs, a prototype is produced and

improved PQ efficiency of the proposed EV charger is achieved.

## 2. Literature Survey

C. K. and C. Chau, "Electric Vehicle power electronics challenges," in *Proc. Despite the increasing concern for energy efficiency and environmental safety, the advancement of electric vehicle technology has advanced at an accelerated pace. The 1990s were promising for realistic, affordable electric vehicles to come to life as the decade progressed. The paper discusses the current state of electric vehicle propulsion systems with focus on how the advancement of electric motors and power electronics have affected electric vehicle propulsion systems. The problems of power electronics in the sense of electric vehicle charging, electric brake systems and other important applications are discussed. The future potential of electric vehicles is addressed, as well as their effects on the market.*

B. A Fayed and Tars, "Overview of fundamental principles of battery chargers" This paper provides a summary of the fundamentals of battery chargers as they pertain to charging methods and the circuits that enforce these charging methods. Next, we will cover open circuit, discharging, and charging operations of batteries. First, it is illustrated how in general pulse charging is applied. The CCCV charging scheme is outlined and circumstances where CCCV charging could be acceptable are defined. The paper addresses the various methods of applying the CCCV charging scheme (linear and switching), and then adds cell balancing, cell gauging, and multi cell chargers to the mix.

M. Yan and Palmer. This paper analyzes the main ways of charging batteries to plug-in electric and hybrid vehicles. 28, 5, pp. 2141-2168, May 2013. This article focuses on the current state of electric vehicle charging technologies and the experience of drivers driving electric vehicles. The chargers are usually categorized into AC types and DC types. This device removes interconnection issues and needs little hardware. Wireless power would allow the power grid to pass electricity back to the customer. On-board chargers are used because of financial, weight, and space constraints. In combination with the electric motor, stopping these issues altogether is feasible. Their availability reduces on-board storage requirements and the cost of using them. On-board power chargers are either inductive or conductive An offboard charger can run at high charging rates and is comparatively smaller than the internal charging system. Three different power levels are compared and defined. Issues like land-consuming are tackled Evaluated and compared based on how much energy they put out, how fast they charge, where they charge, how much they pay, and how well they work.

S. S. Williamson, A. K. Rathore, and F. Whelan. Sketchenstein In this article, the latest developments in the industrial electronics industry in the field of transportation

electrification, and systems that use this technology. The paper focuses on the different aspects of electric and plug-in hybrid vehicles and the systems that are necessary for proper operation. The paper deals with energy storage problems for electric vehicles as well as charging and drive mechanisms for our electric cars. The value of voltage equalization in lithium-ion batteries, and how it can improve the life of lithium-ion batteries. Furthermore, a comparative analysis of EV/PHEV battery charger discrimination is given. Several traditional charging system approaches and DC to DC methods are checked. Various alternative architectures for electric vehicle propulsion systems and powerful bidirectional DC/DC converter topologies are highlighted. Novel modulation strategies for hybrid electric vehicles are also discussed. The architectures that are based on the unique characteristics of the battery.

F. Musavi, Eberle, Edington and Eberle G. Dunford, "Evaluation and Efficiency Comparison of Front End AC-DC Plug-in Hybrid Charger Topologies," As a key component of a plug-in hybrid electric vehicle (PHEV) charging system, performance and efficiency of the ac-dc converter are critical. The study focuses on a number of electric vehicle battery chargers topologies. The paper discusses several boost converter designs that deliver high performance, high power factor, high density, and low cost. Experimental results are presented, along with a comprehensive discussion of each one. This design is best for residential level I charging in the United States where the average supply is limited to 120 volts and 1,440 watts. When it comes to residential level II applications, bridgeless interleaved PFC boost converters make the most sense for power supplies that deliver 3.3kW, 5kW, and 6.6kW ratings.

H. Cho, "Interleaved Coaxial Buck-Boost Power Factor Correction (PFC) Converter," A system with a power factor correction and high performance is suggested for the entire load range. The adaptive master-slave interleaving mechanism ensures that the motors remain in synchronization despite transients occurring during transmission. By increasing the number of parallel-connected buck converters, the ripple on the input current is significantly decreased, and the ripple frequency is doubled, which leads to narrower differential mode current filters. The different harmonics are tuned until the appropriate output voltage range is discovered. The circuit is improved to run on a 300 W prototyped, and is tested on an 80 V output. The output of the power unit remains above 96% down to as low as 20% under all conditions. Even at 10% of the full load, the output remains above 94%. The input current harmonics are IEC accepted standards.

### 3. Bridgeless Cuk Converter Topology Supported EV - Charger

#### A) CONFIGURATION AND OPERATION:

The characteristics and operation of proposed power quality enhanced electric vehicle charging stations are outlined in figures. The PV is connected to BL cuk converter through inverter, During the positive portion of the cycle, the cell Li-S-Do-Lo is in action. However, during negative half-cycles the second Cuk cell, Li2-S2-Do2-Lo2-Dn, is involved. The inductors are chosen for the Cuk converter cells to function in CCM. However, to ensure that output inductors L1 and L2 are built such that the converter enters DCM when the current reaches zero. The voltage between the two capacitors is such that it remains constant throughout the switching period. As stated, both switches S1 and S2 use the same PWM signal, which reduces the cost and circuit complexity of the final system.

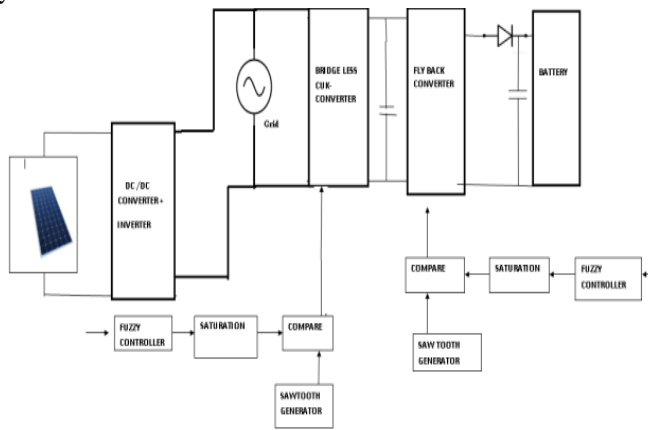


Figure .2 Proposed BL Cuk Converter based on PV integrated EV Charger Configuration

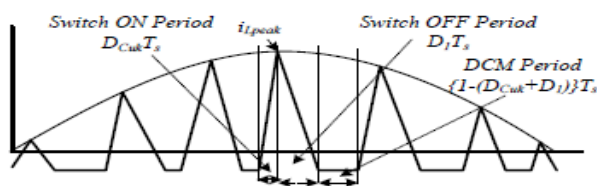


Fig .3 PFC Operational Policy

The voltage regulation of the PFC voltage converter is done through a single voltage feedback control loop. The flyback converter is designed to work with a cascaded controller, which allows the voltage to swing between CC and CV while charging. Figure.2 explains how inductor current behaved in DCM PF correction, and how the Cuk converter worked in the range of activity.

#### Operation of BL Cuk PFC Converter:

Only the positive half-cycle of the BL converter is used, as shown in the pictures (4, A) . (c). This section describes the functionality of the proposed EV charger, and the efficiency of the Cuk converter.

The modes for Mode P-I are shown in Fig. At Time  $t = 1$ , the first mode of positive half-cycle operation starts when the switch S 1 is switched on by the gate pulse. The current through the input inductor increases linearly with increases in voltage. current flows from positive wire diode Dp to negative wire diode Dp which is in conducting state. The overall change waveform modes are shown in Figure. The voltage across the capacitor begins decreasing through the switch, and the output inductor, providing the necessary amount of current. The system retains its positive output voltage regardless of whether the voltage is present at the capacitor.

The maximum current stress experienced by switch S1 in this mode is given as (current and capacitor capacitances).

$$I_{s1pk} = \frac{V_{spk} D_{cuk} T_s}{L_{eq}} \tag{1}$$

Where the  $L_{eq}$  represents the real value of the circuit inductance, and the sum of the main and secondary inductances for the proposed circuit.  $V_{spk}$  is the highest AC voltage that can be input to the AC outlet,  $D_{cuk}$  is the total amount of time that S1 is on, and  $T_s$  is how long it took to turn on.

Mode P-II [turn OFF time,  $D_{cuk} T_s \leq t \leq D_1 T_s$ ] starts following the turn OFF of switch S1 at instant t. As Li1 starts to release its stored energy in the inductor, the voltage begins to increase around the capacitor as the diode begins to conduct. 6 . (b) The output inductor, L1, releases stored energy due to the current in the circuit by the diode, and the capacitor, respectively.

The current is calculated flowing through the current generator  $i_{Lo1}$ .

$$\frac{di_{Lo1}}{dt} = \frac{V_{cuk}}{L_{o1}} \tag{2}$$

Where, the voltage output of the BL Cuk converter is BL Cuk.

As the current flowing through the rectifier, the moment the current loses its full value, hits zero. The duty cycle of this switching mode can be calculated by following these basic instructions.

$$D_{cuk} T_s + D_1 T_s \leq T_s \text{ which gives, } D_{cuk} + D_1 \leq 1 \tag{3}$$

In operating mode II, proposed Cuk converter.

$$V_{cuk} T_{off} = n T_{on} V_s$$

$$T_{off} = \frac{n T_{on} V_s}{V_{cuk}} \tag{4}$$

To measure the switching time, where n is the conversion ratio,  $T_s$  is the switching period,  $T_{on}$  and  $T_{off}$  is the turn ON and OFF times. For isolated card Cuk converter  $Cuk$   $n=1$ . Since  $V_{ses} = V_{spk} \sin \omega t$ , and DC gain is  $M = V_{Cuk} / V_{spk}$ , it follows.

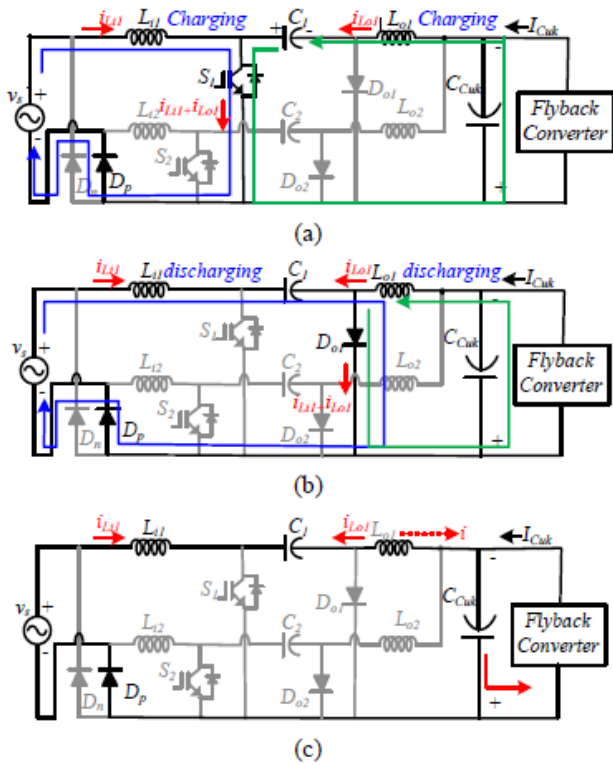


**Fig .4 EV Circuit Performance Charger with BL PFC Cuk Converter during a good half cycle (a) Mode P-I (b) Mode P-II (c) Mode P-III**

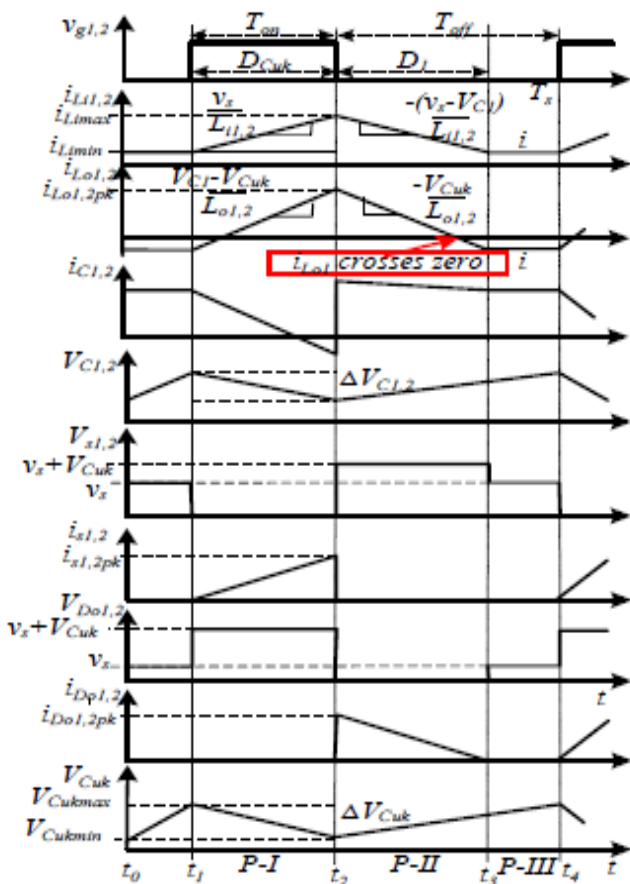


**Fig .5 The corresponding behavior of a variety of transitions over the entire transition cycle**

The relation in (4) is modified as,

$$D_1 T_s = \frac{n D_{cuk} T_s}{V_{cuk}} (V_{spk} \sin \omega t)$$

$$D_1 = \left( \frac{n D_{cuk}}{M} \right) \sin \omega t \tag{5}$$

In rad/sec, the corner frequency given as  $2\mu/T_s$  is denoted by  $\omega_s$ .

Mode P-III: this mode is called a DCM mode whereby input current to the circuit is zero. Mode is called a DCM mode. The power output is the same as the current input. The current must be reversed in order to control this circuit through one of the inductors (the "output inductor" here). 5-6(c) or before mode-II ends, it becomes 0. A constant flow passes through the circuit in the present example. 6. A sequence of alternating values I and I is becoming the current of the inductors. The intermediate condenser is still loaded via the input and exit diode and was not fully loaded at first.

The DC-link condenser's flyback converter receives the necessary power from the optional CCuk condenser. The power output, the inductor, decides the amount of time the DCM is working.

The peak current is increased as the inductance decreases and hence the length of the DCM is longer. The disrupted driving mode is typically represented as,

$$t_3 - t_4 = T_s - \{(t_2 - t_1) + (t_3 - t_2)\}. \tag{6}$$

At the end of the negative half-line the same switching sequence is repeated and the next operation cycle begins.

**4. Proposed Control Manager**

**The proposed charger control strategy is described below. Control of Bridgeless PFC Converter**

The BL PFC converter operates in intermediate drive, an operation mode designed to be controlled using the voltage tracker mode. The voltage tracking control is implemented by a fluid controller which configures the current of the input voltage according to the maximum output from the BL converter. To detect the occurrence of a sudden voltage change and warn the user, a voltage sensor is used. A voltage measured is compared to a reference voltage ( $V_{Cukref}$ ). The voltage V error on the voltage feedback controller is achieved. The error is represented as a plus or minus during each sampling moment.

$$V_{cuke}(n) = V_{cukref}(n) - V_{cuk}(n). \tag{7}$$

A PWM dependent comparator output changes the duty cycle to generate the right output voltage at the same time as Fuzzy controllers processing. The pulse is equivalent to the high frequency wave in PWM comparators, which results in the output of pulses for a BL PFC converter.

$$\text{For } v_s > 0; \text{ or } v_s < 0; \text{ If } S_c < C_{vcuk} \text{ then } S_{1,2} = 1$$

$$\text{If } S_c \geq C_{vcuk} \text{ then } S_{1,2} = 0 \tag{8}$$

The proposed BL Cuk converter is the result because the PWM pulse is passed between two switches. A DC connection voltage is obtained over the broad mains voltage



range and regulated through the acceptable duty cycle limit. As a result, single-voltage-sensor control strategy is simple compared to other converters based on the continuous conduction mode.

The novelty of the proposed control is observed because for both half-cycles of the converter the control circuit is the same.

In order to mitigate the loss of conduction through the inactive body diode, both switches S1 and S2 work simultaneously with a normal driver signal, these are called partial.

**TABLE II. DESIGN RESULTS OF PROPOSED CHARGER**

Components	Specifications
Input Inductance, $L_{i,2}$	4mH
Output Inductance $L_{o1,2}$	150μH
Intermediate Capacitor $C_{1,2}$	3μF
Magnetizing Inductance, $L_f$	130μH
Transformer Turns ratio	0.333
DC-link Capacitor $C_{Cdk}$	2000μF,400V
Battery Specifications	48V, 100Ah
Charger Output Capacitor $C_{Cdk}$	2000μF,100V

The driver is provided with the same driver signal, which prevents losses during the respective halves in the driver's corporal diode.

**Control of Flyback Converter**

At the output, the PI and FUZZY controllers are used by the flyback converter to keep CC charging even during voltage changes. For a motor speed control, a constant reference voltage compares the sum of electrical energy in the battery. The voltage is supplied to a PI controller by the ambient unit. At a maximum charge current limit, which sets the reference current of the inner current loop, the output produced by the PI controller is saturated. The equations are given for the error voltage and for a correction of the fixed voltage in the kth sample case.

$$V_{batte}(n) = V_{batt}^*(n) - V_{batt}(n) \tag{9}$$

The voltage parameters are A and Vb. However, this reference value is contrasted with the sensed charging current, and the resulting error is sent to the current of the internal controllers. The PI controller loop will be inactive if the target output voltage is saturated by the value of the referral charging current. In comparison of the Fuzzy control output with a sawtooth wave, the PWM generator block is used to calculate the pulses required. The wrong load control signal is defined as,  $I_{batt}$  and the right charge signal,  $CI_{batt}$ .

$$I_{batt}(n) = I_{batt}^*(n) - I_{batt}(n) \tag{10}$$

Therefore k are new FUZZY controller parameters as an instant of contrast sampling and  $I_{bats}$ . Signal processing, accompanied by a PWM comparator, provides the required

PWM values. The same pulses (input and output) are generated in the comparator with a

high frequency carrier wave by the pulse-width modulated comparator (PWM).

$$S_f \text{ is "ON," otherwise } S_f \text{ is "OFF"}$$

$$\{\text{if } Md < CI_{batt}, \text{ the } s_f \text{ is 'ON'} \tag{11}$$

The charger will then switch from PWM to the CV mode as soon as the battery reaches 80 percent SOC. The voltage regulator in this mode follows the constant voltage relation, and the loading loading period is completed by 100% SOC. The battery is fully charged at the end of every cycle and the amount of current drawn from the source is reduced to a low value. The motorcycle works in a constant voltage mode.

**5. Proposed Fuzzy Logic Controller**

With the aid of a design professional, Fuzzy logic controller improves conventional device design. With fuzzy logic, robust mathematical modelling in control processes can be greatly reduced. A human operator can monitor a process much more efficiently than a controller based on modern analytical techniques.

In recent years FLC's implementation of fluid set theory has become popular. A fuzzy set is a subset of sets where only two separate values, 0 to 1, are inferred by the membership function (MF) values. The following is a fuzzy package.

A fuzzy set A in discourse universe U is defined by a member function  $A(x)$  which at the interval of A measures member status [0, 1] and at that interval associates  $A(x)$  number with each element x of U.

Fuzzy logic regulation is seen as actual physical structure and logic. 6 concerns all four of the main parts of (1) fuzzy source code, (2) knowledge base, (3) engine inference, and (4) defluence.

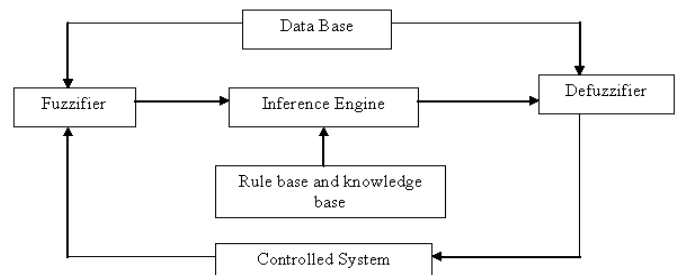


**Fig.6 Structure of Fuzzy Logic controller**

**1. Fuzzification:**

Maps from the original semantime to fluid collection capturing other realms of discourse. For a given value x, the membership intensity in subcatégor A is mapped. (x). (x). The process of flushing consists of the next steps. Tests the variables' influence.

1. Computers adjust the range and map new range into the respective universe of discourse for each of the input variables.

2. Conducts the fluctuation function, which converts input data into suitable language variables that can be interpreted as fluorescent sets labels.

**2. Knowledge Base (KB):**

The basis of knowledge consists of the meanings and the control rules that describe when, how and why you apply the fuzzy control rules, of the fuzzy MFs for the input and output variables.

A database and language rules base are included in the framework.

1. The database serves as a reference for language control principles and pointless data processing.

2. The basic rule is structured to identify control goals and controls for domain experts through a set of language rules.

**3. Inference Mechanism:**

Decision making on pen and paper using a set of fluid if then rules like:

$$IF X = A = Y = B = B = C.$$

The linguistic values for x, y and z, a, b, and c represent two variables of input and one variable of power.

It is a cornerstone of an FLC, capable of simulating human existence, including its decision making on the basis of furious logic and the rules of inference of furious logic.

Generally speaking, fuzzy sets are mapped to a pair of outputs, the laws between the two systems.

**4. Defuzzification:**

Defuzzification is used to measure linguistic-dependent numerical values. In this study, the center method was used.

(1) A mapping scale that translates the input value range to the output variable set of values.

(2) Defluence, an approach to differentiate between non-fuzzy control behavior and a fluctuating control operation.

**6. Simulation Results**

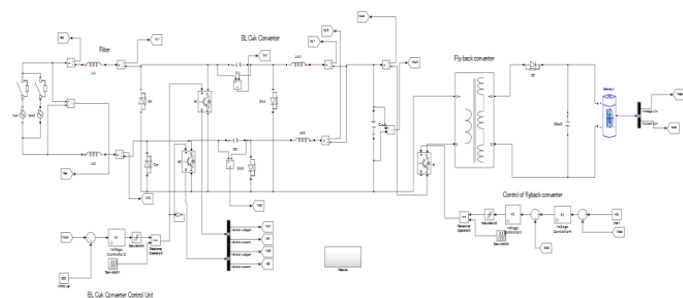


**Fig 7 MATLAB / SIMULINK diagram of the proposed BL Cuk Charger Adjustment**

**Case 1: Simulation results under steady state for proposed EV charger**

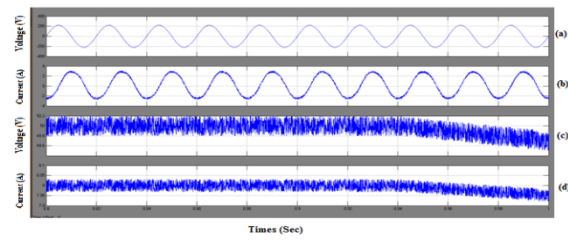


**Fig.8 Source and Battery side quantities (a)Mains voltage (b)Mains current (c)Battery voltage (d)Battery current**

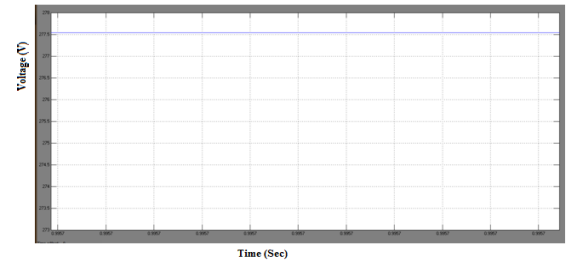


**Fig.9 DC PFC converter power link**

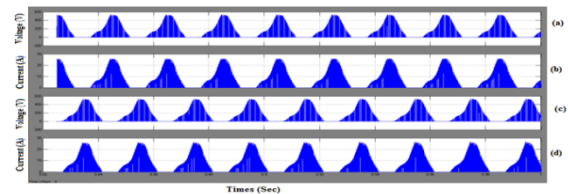


**Fig .10 Change voltage and no current output effect on current PFC (a) Change voltage Vs1 (b) Change current is1 (c) Change voltage Vs2 (d) Change current is2**

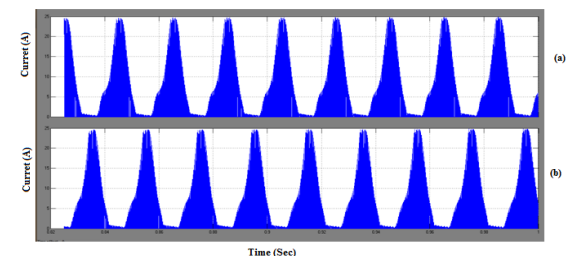


**Fig.11 Output inductor current (a) i\_o1 (b) i\_o1**

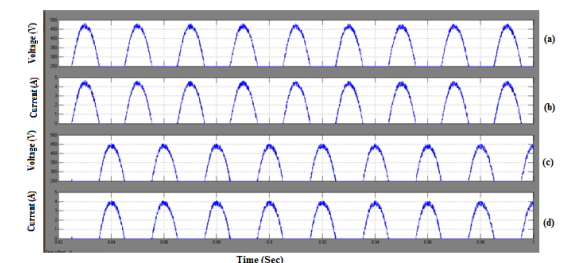


**Fig .12 charging voltages capacitor to CCM (no current return on Li1 and Li2 in -ve no + ve half respectively) (a) Capacitor voltage V\_c1 (b)Input inductor current I\_L1 (c) Capacitor voltage V\_c2 (d) Input inductor current I\_L1**

**Case-2: Performance of Charger at Wide Fluctuations in Input Voltage**

**A) Charger performance during 50% fluctuation in mains voltage ;Charger performance from 220V-110V**

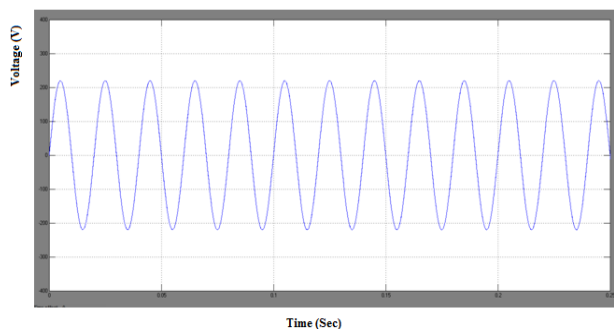


**Fig .13 AC mains voltage**

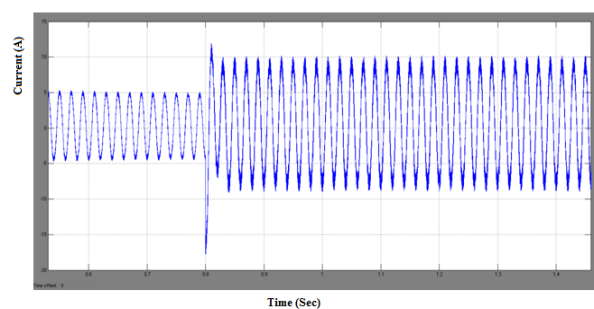


**Fig.14.Mains current increased AC mains current**

**B) Charger performance during 50% variation in power consumption; Charging performance from 110V- 220V**

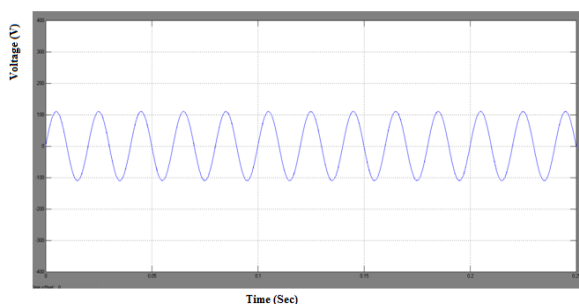


**Fig.15 Mains voltage**

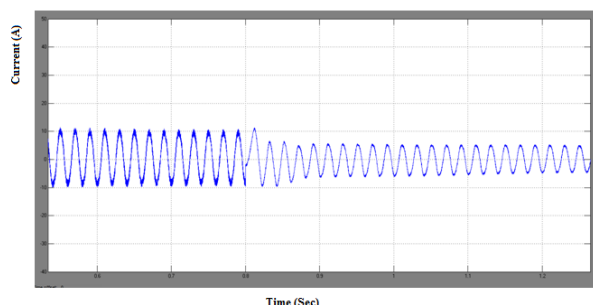


**Fig.16Mains current**

**Case 3: Improved power quality parameters in AC Mains**

**A) Improved energy quality on source power**

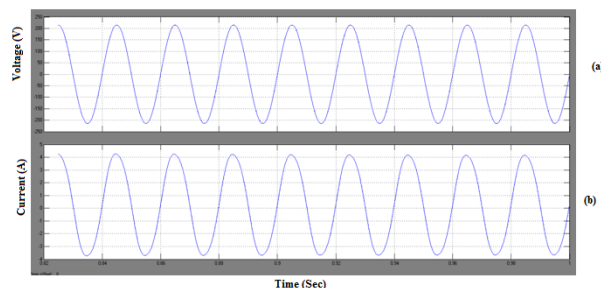


**Fig.17(a)Mains voltage (b)Mains current**

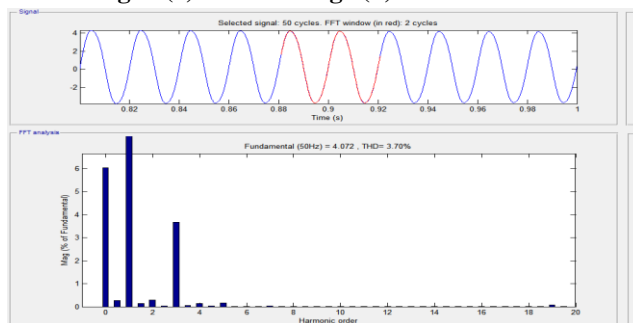


**Fig .18 THD of source voltage = 3.70%**

**B) Improved Power Quality for sudden dip in source voltage**

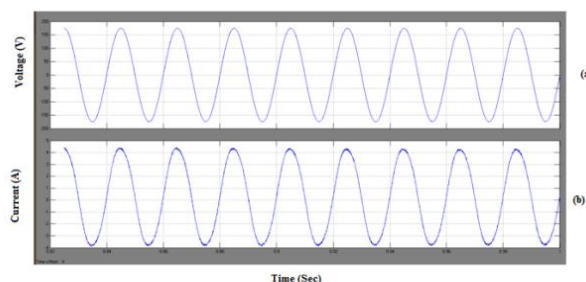


**Fig .19 (a)Mains voltage (b)Mains current**

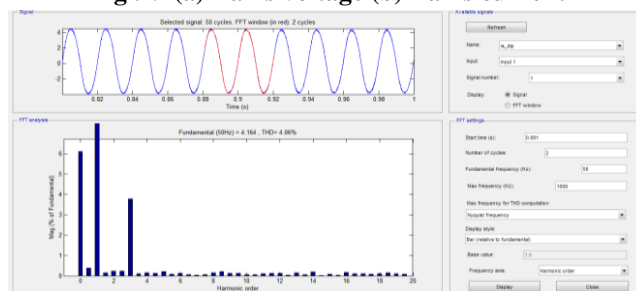


**Fig .20 THD of source voltage ( sudden dip in source voltage) = 4.06%**



**C) Improved Power Quality for sudden rise in source voltage**

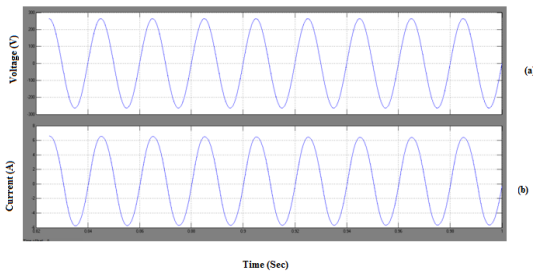


**Fig .21.(a)Mains voltage (b)Mains current**

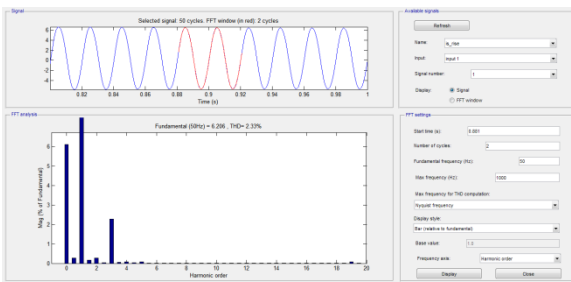


**Fig .22.THD of source voltage (sudden rise in source voltage)= 2.33%**

**EXTENSION RESULTS**

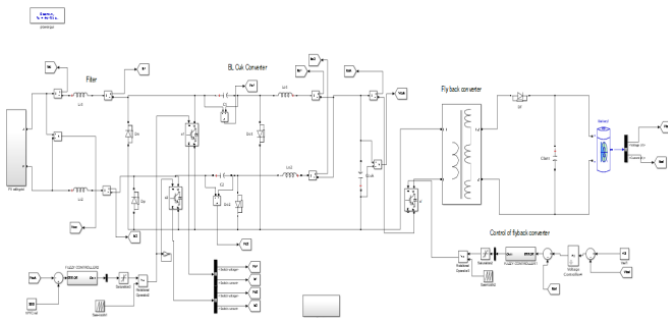


**Fig .23 MATLAB / SIMULINK diagram of Proposed PV integrated Electric Vehicle (EV) charger (battery) by adopting Bridge Less (BL) Cuk converter with logic controller.**

**Case 1: Simulation results under steady state for proposed EV charger**

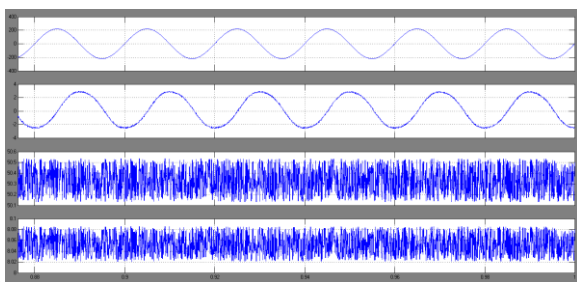


**Fig .24 Source and Battery side quantities (a)Mains voltage (b)Mains current (c)Battery voltage (d)Battery current**

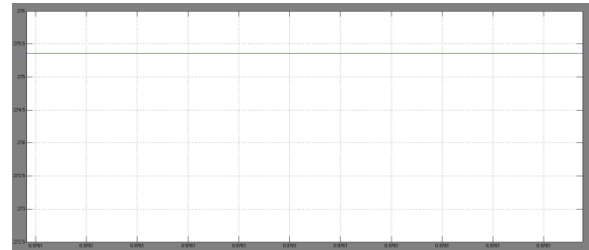


**Fig . 25 DC link voltage of PFC converter**

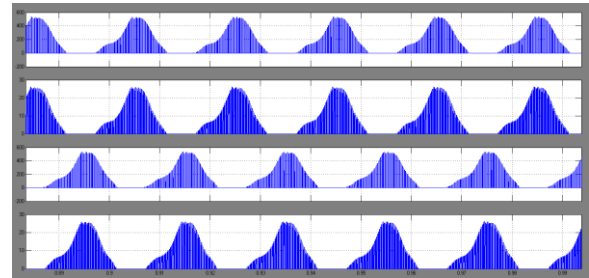


**Fig 26. Switch voltage and No circulating current effect on PFC Current (a)Switch voltage  $V_{s1}$  (b)Switch current  $i_{s1}$  (c)Switch voltage  $V_{s2}$ (d) Switch current  $i_{s2}$**

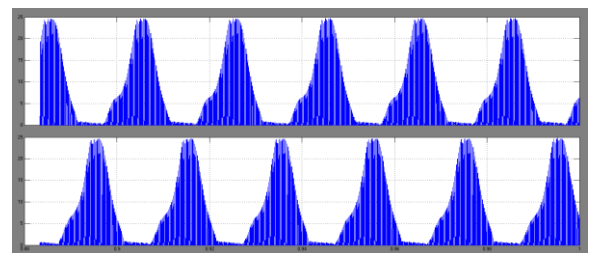


**Fig 27. Output inductor current (a) $i_{o1}$  (b)  $i_{o1}$**

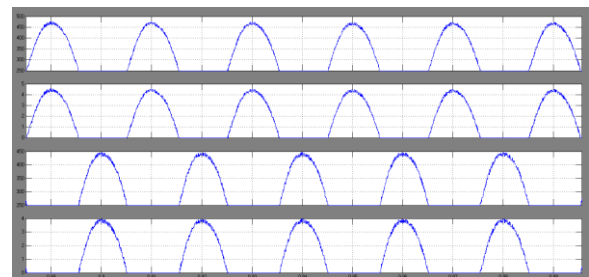


**Fig 28. charger Capacitor voltages in CCM (no return current through Li1 and Li2 in -ve and +ve half respectively (a) Capacitor voltage  $V_{c1}$  (b)Input inductor current  $I_{L1}$  (c) Capacitor voltage  $V_{c2}$  (d) Input inductor current  $I_{L1}$**

**Case-2: Charger Performance at Wide Variation in Input Voltage**

**A) Charger performance during 50% variation in power consumption; Charging performance from 220V-110V**

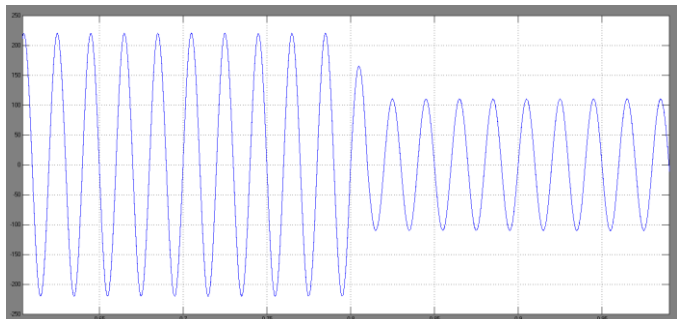


**Fig. 29. AC mains voltage**

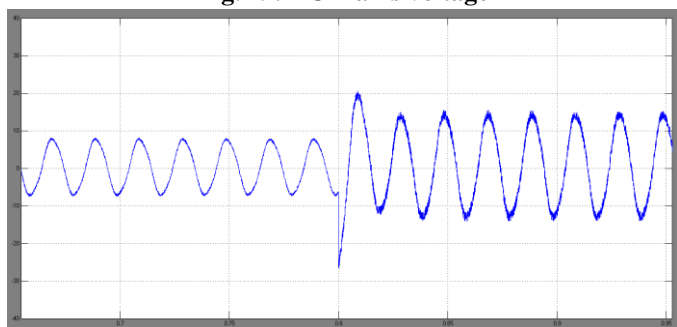


**Fig.30 Mains current increased AC mains current**

**B) Charger performance during 50% fluctuation in mains voltage ;Charger performance from 110V- 220V**

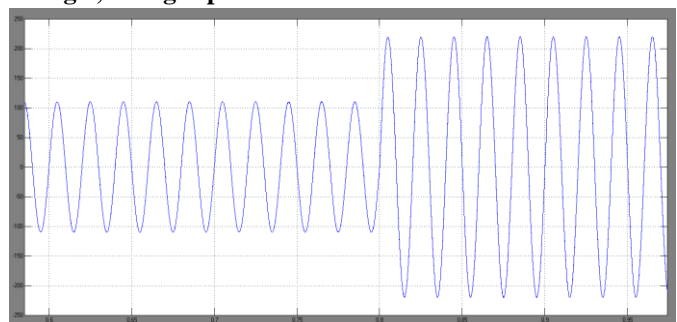


**Fig 31.Mains voltage**

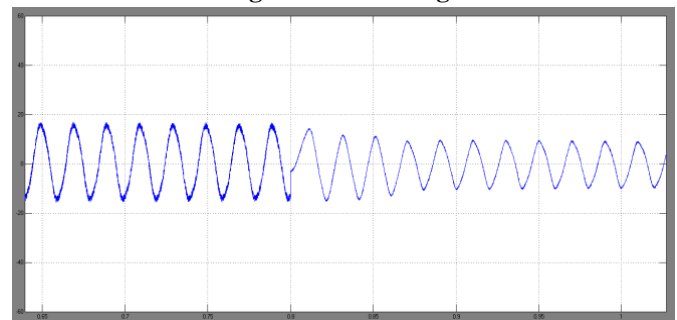


**Fig 32. Mains current**

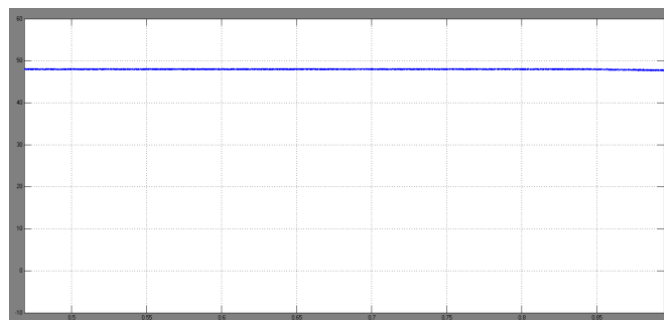


**Fig 33. Battery voltage**

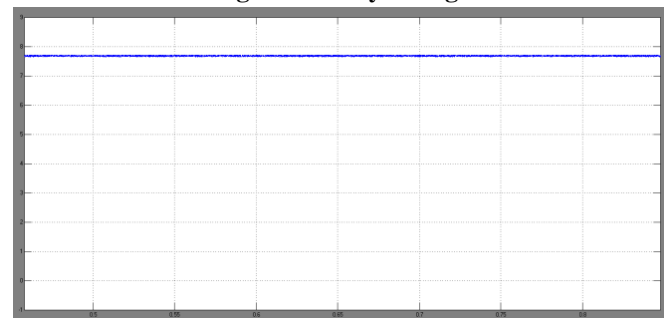


**Fig 34. Battery current**

**Case 3: Improved power quality parameters in AC Mains**

**A) Improved Power Quality at nominal source voltage**

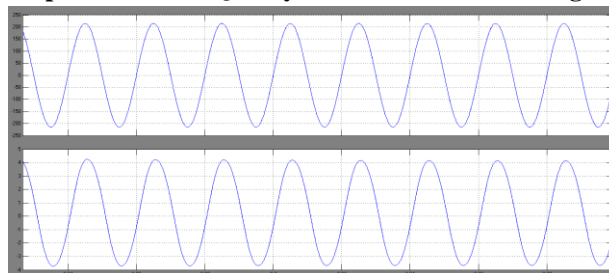


**Fig 35. (a)Mains voltage (b)Mains current**

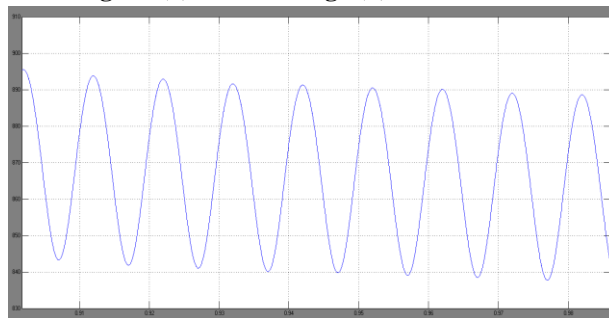


**Fig 36. (a)Active power**

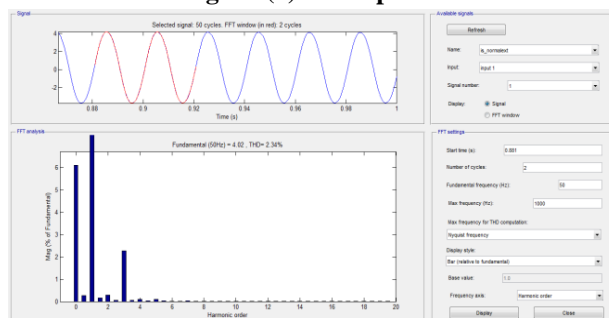


**Fig 37. THD of source voltage = 2.34 %**

**B) Improved Power Quality for sudden dip in source voltage**

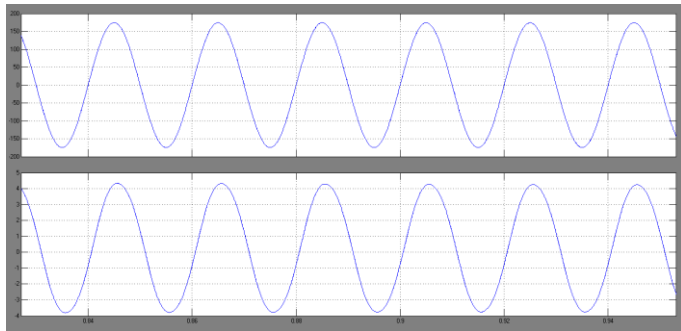


**Fig 38. (a)Mains voltage (b)Mains current**

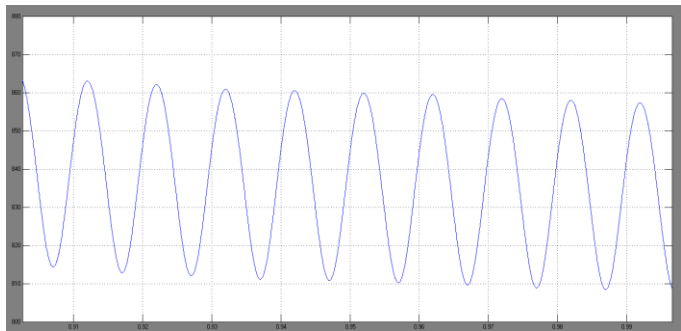


**Fig 39. (a)Active power**

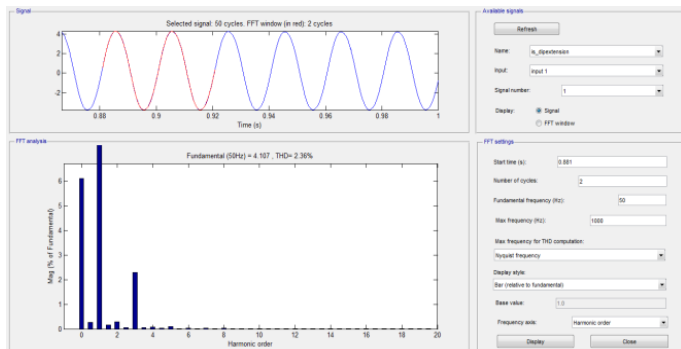


**Fig 40. THD of source voltage ( sudden dip in source voltage) = 2.36%**

**C) Improved energy quality of sudden increase in electrical power**

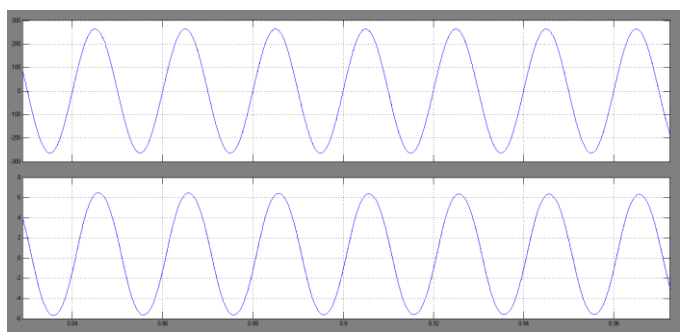


**Fig 41.(a)Mains voltage (b)Mains current**

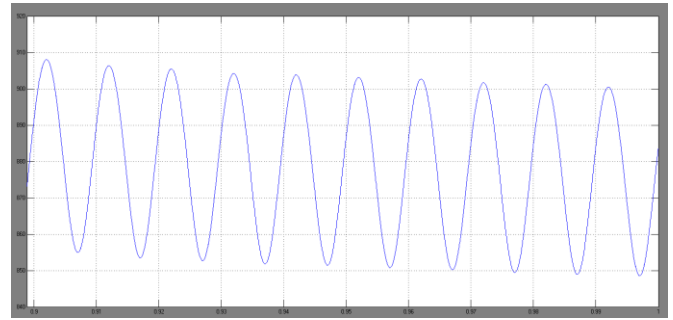


**Fig 42.(a)Active power**

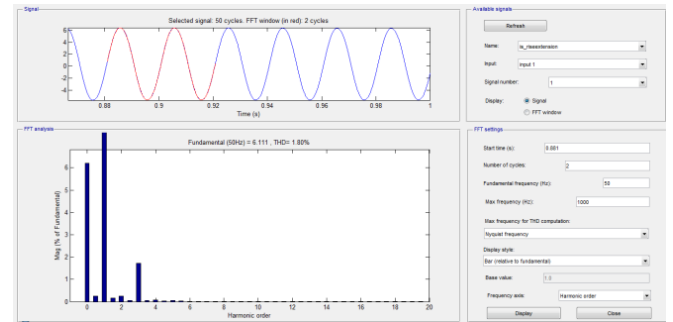


**Fig 43. THD of source voltage (sudden rise in source voltage)= 1.80%**

**Comparison table**

State of voltage	THD of current with PI controller	THD of current with fuzzy controller
At nominal source voltage	3.70%	2.34%
Sudden dip in the source of energy	4.06%	2.36%
Sudden rise in source voltage	2.33 %	1.79%

**7. Conclusion**

The BL Cuk converter has fewer conduction components during the single switching period and a more efficient Transient Quasi-Static Electric Loader. The proposed PFC-Cuk converter offers improved PFC features, and reliable DCM operation. As a consequence, the charger is reduced in size. The potential advantage of the proposed topology is that it avoids unnecessary coupling circuits and prevents the inactive switch from being transmitted through a body diode. This aids the loader's efficiency even further. In stable state and at least a 50% voltage difference between the grid and battery, the charger demonstrated adequate charging characteristics. The proposed charger is tested using the PQ method in accordance with IEC 61000-3-2 guidelines. The proposed charger provides the benefit of increased quality and reliability of electricity by better charging.

## References

- [1] C. Chan et.al., "Power electronics challenges in electric vehicles," in Proc. IEEE IECON'93., pp. 701–706.
- [2] B. Tar et.al., "An overview of the fundamentals of battery chargers," IEEE MWSCAS'16, pp. 1-4.
- [3] M. Yilmaz et.all, "Review of battery charger topologies, charging power levels, and infrastructure for plug-in electric and hybrid vehicles," IEEE Transactions Power Electronics, vol. 28, no. 5, pp. 2151–2169, May 2013.
- [4] S. S. Williamson et.all., a "Industrial electronics for electric transportation: Current state-of-the-art and future challenges," IEEE Transactions Industrial Electronics, vol. 62, no. 5, pp. 3021–3032, May 2015.
- [5] Limits for Harmonics Current Emissions (Equipment current per Phase), International standards IEC 61000-3-2, 2000. 16A □
- [6] F. Musavi et.all., "Evaluation and Efficiency Comparison of Front End AC-DC Plug-in Hybrid Charger Topologies," IEEE Transactions Smart Grid, vol. 3, no. 1, pp. 413-421, March 2012.
- [7] H. Choi et.all., "Interleaved Boundary Conduction Mode (BCM) Buck Power Factor Correction (PFC) Converter," IEEE Transactions Power Electronics, vol. 28, no. 6, pp. 2629-2634, June 2013.
- [8] Y. Hsieh et.all., "An Interleaved Boost Converter With Zero-Voltage Transition," IEEE Transactions Power Electronics, vol. 24, no. 4, pp. 973-978, April 2009.
- [9] C. Li et.all., "Family of Enhanced ZCS Single-Stage Single-Phase Isolated AC–DC Converter for High-Power High-Voltage DC Supply," IEEE Trans. Ind Electron., vol. 64, no. 5, pp. 3629- 3639, May 2017.
- [10] S. Chen et.all., "Analysis and Design of Single- Stage AC/DC SLLC Resonant Converter," IEEE Transactions Industrial Electronics, vol. 59, no. 3, pp. 1538-1544, March 2012.
- [11] S. Lee et.all., "High-Efficiency Soft-Switching AC–DC Converter With Single-Power-Conversion Method," IEEE Transactions Industrial Electronics, vol. 64, no. 6, pp. 4483-4490, June 2017.
- [12] D. H. Kim et.all., "An integrated battery charger with high power density and efficiency for electric vehicles," IEEE Trans. Power Electron., vol. 32, no. 6, pp. 4553- 4565, June 2017.
- [13] Chuan et.all., "A single-phase integrated onboard battery charger using propulsion system for plug-in electric vehicles," IEEE Trans. Veh. Technol., vol. 66, no. 12, pp. 10899-10910, Dec. 2017.
- [14] M. M. Jovanovic et.all., "State-of-the-art, single-phase, active power-factor-correction techniques for high-power applications—An overview," IEEE Trans. Ind. Electron., vol. 52, no. 3, pp. 701–708, Jun. 2005.
- [15] L. Petersen et.all, "Two-stage power factor corrected power supplies: The low component-stress approach," in Proc. IEEE APEC, 2002, vol. 2, pp. 1195–1201.
- [16] Bhim Singh et.all., "A review of single-phase improved power quality AC-DC converters," IEEE Transactions Industrial Electronics, vol.50, no. 5, pp.962-981, July 2003.
- [17] B. Zhao et.all., "Family of bridgeless buck-boost PFC rectifiers," IEEE Transactions Power Electronics, vol. 30, no. 12, pp. 6524-6527, Dec. 2015.
- [18] R. Kushwaha et.all., "An Improved Battery Charger for Electric Vehicle with High Power Factor," in Proc. IEEE IAS Annual Meeting, 2018, pp. 1-8.
- [19] D. S. L. Simonetti et.all., "Design criteria for SEPIC and Cuk converters as power factor preregulators in discontinuous conduction mode," in Proc. International Conference on Industrial Electronics, Control, Instrumentation, and Automation, 1992, pp. 283-288 vol.1.
- [20] A. A. Fardoun et.all., "New efficient bridgeless Cuk rectifiers for PFC applications," IEEE Transactions Power Electronics, vol. 27, no. 7, pp. 3292- 3301, July 2012.
- [21] M. R. Sahid et.all., "A bridgeless Cuk PFC converter," in Proc. IEEE IAPEC, 2011, pp. 81-85.
- [22] A. J. Sabzali et.all., "New Bridgeless DCM Sepic and Cuk PFC Rectifiers with low conduction and switching losses," IEEE Transactions Industry Applications, vol. 47, no. 2, pp. 873-881, March-April 2011.
- [23] M. Mahdavi et.all, "Bridgeless CUK power factor correction rectifier with reduced conduction losses," IET Power Electronics, vol. 5, no. 9, pp. 1733-1740, November 2012.
- [24] R. Kushwaha et.all, "A power quality improved EV Charger with bridgeless Cuk converter," in Proc. IEEE PEDES 2018, pp. 1-6.
- [25] A. Jha et.all, "Bridgeless Zeta PFC converter for low voltage high current LED driver," in Proc. IEEE CERA, 2017, pp. 539-544.
- [26] SAE Electric Vehicle and Plug-in Hybrid Electric Vehicle Conductive Charge Coupler, SAE Std. J1772, 2010.